Dynamic Loads in Parallel Shaft Transmissions — Part 2

Hsiang-Hsi (Edward) Lin, Memphis State University, Memphis, TN;
Ronald L. Huston, University of Cincinnati, Cincinnati, OH;
John J. Coy, NASA Lewis Research Center, Cleveland, OH

AUTHORS:

DR. HSIANG HSI LIN *is on the faculty at Memphis State University. His research includes kinematics, dynamics, optimization, finite element methods, and computer-aided design and analysis of mechanical systems. He received his undergraduate degree from National Chung Hsing University and did his graduate work at the University of Cincinnati.*

DR. RONALD L. HUSTON *is Professor of Mechanics at the University of Cincinnati and Director of the University's Institute for Applied Interdisciplinary Research. He earned his degrees in Mechanical Engineering and Engineering Mechanics from the University of Pennsylvania.*

DR. JOHN J. COY *is Branch Chief, Rotorcraft Systems Technology in the Propulsion Systems Division at NASA Lewis Research Center in Cleveland, OH. He took his degrees in Mechanical Engineering from the University of Cincinnati. He is the author of numerous papers and is a member of ASME. Dr. Coy is a licensed professional engineer in the State of Ohio.*

Summary:

Solutions to the governing equations of a spur gear transmission model, developed in a previous article are presented. Factors affecting the dynamic load are identified. It is found that the dynamic load increases with operating speed up to a system natural frequency. At operating speeds beyond the natural frequency the dynamic load decreases dramatically. Also, it is found that the transmitted load and shaft inertia have little effect upon the total dynamic load. Damping and friction decrease the dynamic load. Finally, tooth stiffness has a significant effect upon dynamic loading: the higher the stiffness, the lower the dynamic loading. Also, the higher the stiffness, the higher the rotating speed required for peak dynamic response.

Introduction

The development of a simple parallel shaft spur gear transmission model with its dynamic differential equations and solution procedures were presented in Reference 1. Various parameters such as inertia, stiffness, friction, and damping were included in the governing equations for further study.[1]

The purpose of this report is to determine the effect of these parameters on gear dynamic load. The dynamic load of a gear transmission can be found by solving the governing equation. The solution is known as the dynamic motion of the gear transmission. This dynamic motion can then be substituted into other analytical formulae and solved for gear dynamic loads.

A model of the transmission is depicted in Fig. 1. The governing equations are:

$$J_M\ddot{\theta}_M + C_{s1}(\dot{\theta}_M - \dot{\theta}_1) + K_{s1}(\theta_M - \theta_1) = T_M \quad (1)$$

$$J_1\ddot{\theta}_1 + C_{s1}(\dot{\theta}_1 - \dot{\theta}_M) + K_{s1}(\theta_1 - \theta_M) + C_g(t)[R_{b1}\dot{\theta} - R_{b2}\dot{\theta}_2] + K_g(t)[R_{b1}(R_{b1}\theta_1 - R_{b2}\theta_2)] = T_{f1}(t) \quad (2)$$

$$J_2\ddot{\theta}_2 + C_{s2}(\dot{\theta}_2 - \dot{\theta}_1) + K_{s2}(\theta_2 - \theta_1) + C_g(t)[R_{b2}\dot{\theta}_2 - R_{b1}\dot{\theta}_1] + K_g(t)[R_{b2}(R_{b2}\theta_2 - R_{b1}\theta_1)] = T_{f2}(t) \quad (3)$$

$$J_L\ddot{\theta}_L + C_{s2}(\dot{\theta}_L - \dot{\theta}_2) + K_{s2}(\theta_L - \theta_2) = -T_L \quad (4)$$

where J_M, J_1, J_2, and J_L represent the mass moments of inertia of the motor, the gears, and the load; C_{s1}, C_{s2}, and $C_g(t)$ are damping coefficients of the shafts and the gears; K_{s1}, K_{s2}, and $K_g(t)$ are stiffness of the shafts and the gears; T_M, T_L, $T_{f1}(t)$, and $T_{f2}(t)$ are motor and load torques and frictional torques on the gears; R_{b1} and R_{b2} are base circle radii of the gears; t is time; and the overdots indicate time differentiation.

In this report we present the results of numerical solutions of Equations 1 to 4 for a typical transmission system. A flow chart outlining the numerical procedure is presented. Natural frequencies are determined. The dynamic load is determined. Finally, the dynamic factor defined as the ratio of the dynamic load to the static load, is determined.* The results are calculated as functions of the rotating speed and roll angle for a variety of damping and stiffness conditions.

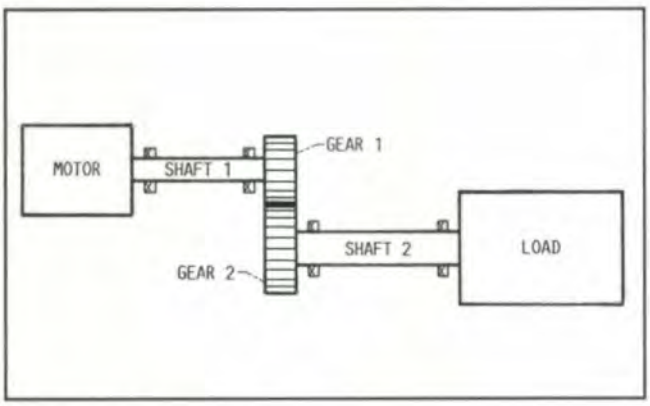

Fig. 1 – A simple spur gear system.

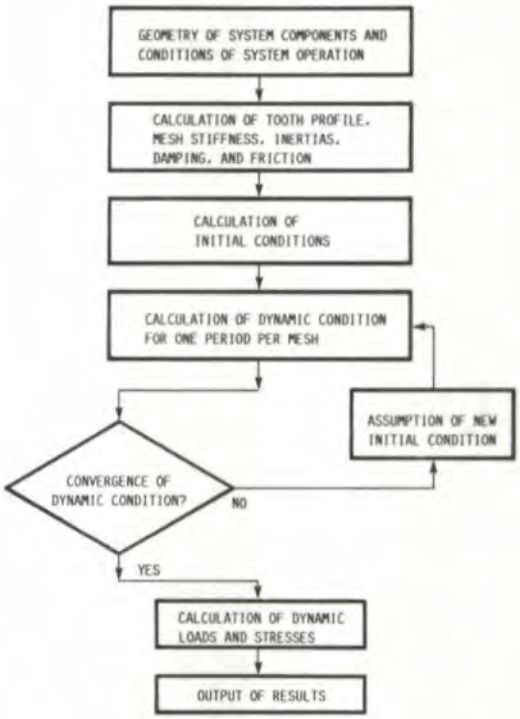

Fig. 2 – Flow chart of computational procedure.

Procedure

Fig. 2 presents a flow chart of the computational procedure used in the parameter study. The procedure is the same as that outlined at the end of Reference 1.

In conducting the analysis it is useful to compare the locations of the peak dynamic loads with the locations of the system natural frequencies (or critical speeds). The natural frequencies themselves may be obtained by examining the undamped equations of motion. These equations may be written in the matrix form:

$$[J]\,[\ddot{\theta}] + [K]\,[\theta] = [0] \qquad (5)$$

where the inertia matrix [J] is

$$[J] = \begin{bmatrix} J_M & O & O & O \\ O & J_1 & O & O \\ O & O & J_2 & O \\ O & O & O & J_L \end{bmatrix} \qquad (6)$$

*The term "dynamic factor" or "dynamic load factor" has been used inconsistently in the literature. The American Gear Manufacturer's Association (AGMA) dynamic factor, K_v, is used as a strength reduction factor and is defined as the maximum static load divided by the maximum dynamic load. This paper will follow the ISO convention, which uses the dynamic factor, K_d, as a load/stress increasing factor. Therefore, $K_d = 1/K_v$.

NOMENCLATURE

- C_g damping coefficient of gear tooth mesh, N-sec (lb-sec)
- C_s damping coefficient of shaft, N-m-sec (in.-lb-sec)
- J_L polar moment of inertia of load, kg-m^2 (in.-lb-sec^2)
- J_M polar moment of inertia of motor, kg-m^2 (in.-lb-sec^2)
- J_1 polar moment of inertia of gear 1, kg-m^2 (in.-lb-sec^2)
- J_2 polar moment of inertia of gear 2, kg-m^2 (in.-lb-sec^2)
- K_d dynamic factor
- K_g stiffness of gear tooth, N/m-rad (in./lb-rad)
- K_s stiffness of shaft, N-m/rad (in.-lb/rad)
- K_v AGMA dynamic factor, Kv = $1/K_d$
- R_b base radius, m (in.)
- R_p pitch radius, m (in.)
- T_L torque on load, N-m (in.-lb)
- T_M torque on motor, N-m (in.-lb)
- T_{f1} torque on gear 1, N-m (in.-lb)
- T_{f2} torque on gear 2, N-m (in.-lb)
- W applied load, N (lb)
- θ angular displacement, rad
- $\dot{\theta}$ angular velocity, rad/sec
- $\ddot{\theta}$ angular acceleration, rad/sec^2
- ω_n natural frequency, Hz
- ξ damping ratio

and the stiffness matrix [K] is

$$[K] = \begin{bmatrix} K_{s1} & -K_{s1} & 0 & 0 \\ -K_{s1} & K_{s1} + (K_g)_{avg} R_{b1}^2 & -(K_g)_{avg} R_{b1} R_{b2} & 0 \\ 0 & -(K_g)_{avg} R_{b1} R_{b2} & K_{s2} + (K_g)_{avg} R_{b2}^2 & -K_{s2} \\ 0 & 0 & -K_{s2} & K_{s2} \end{bmatrix} \quad (7)$$

where $(K_g)_{avg}$ represents the average value of the gear mesh stiffness. It is taken as the sum of the discrete tooth stiffness values of a mesh cycle divided by the number of mesh positions in the cycle.

In the parameter study the system had identical gears with the following properties:

Number of teeth 36
Module, mm . . . . . 3.18 (8 diametral pitch)
Pitch diameter, m (in.) 0.1143 (4.5)
Pressure angle, deg 20
Applied load, N (lb) 2670 (600)
Face width, m (in.) 0.0254 (1.0)
Moment of inertia,
kg m^2 (in.-lb-sec^2) . . 3.3323×10^{-3} (0.02947)
Average tooth stiffness, N m/rad
(lb-in./rad) . . . . . 3.991×10^5 (3.5355×10^6)
Damping ratio 0.10
The shaft stiffness and inertias were:
Shaft stiffness, N m/rad
(in.-lb/rad) 1138.17 (10081)
Load inertia and motor inertia, kg m^2
(in.-lb-sec^2) . . . . 9.989×10^{-3} (each) (0.08841)

Results

Using the aforementioned data in the gear system model shown in Fig. 1, the natural frequencies of the four degrees of freedom model were found to be

$$\omega_{n1} = 0 \text{ (rigid body mode)} \qquad \omega_{n2} = 1.49 \text{ Hz}$$
$$\omega_{n3} = 2.99 \text{ Hz} \qquad \omega_{n4} = 144.8 \text{ Hz} \quad (8)$$

The first three natural frequencies are well below tooth meshing frequencies and are, therefore, not of interest in this analysis (although they can still be excited by shaft eccentricity, which is not modeled here). The fourth natural frequency matches tooth meshing frequency at the critical speed of 8688 rpm, which is within the operating range of the gears.

Fig. 3 shows the variation of dynamic load response for a pair of teeth as a function of roll angle. At speeds much lower than the critical speed, the dynamic load response is basically a static load sharing in phase with the stiffness change, superimposed with an oscillatory load at a frequency corresponding to the natural frequency.

At higher speed, close to the critical speed, the dynamic load variation becomes so abrupt that it produces tooth separation. The peak dynamic load is much higher than the static load and is very likely to be a source of gear noise and early surface fatigue.

Fig. 4 shows the dynamic factor K_d as a function of operating speed. Prominent peaks (resonances) may be seen at speeds of 7650 and 4200 rpm. The larger peak 7650 rpm occurs at 88% of the calculated critical speed. The experimental work by Kubo[6] reported a similar result: that the critical speed was found at about 90% of the calculated critical speed. The second peak at 4200 rpm is a nonlinear effect of the time varying tooth stiffness known as the parametric resonance. This parametric resonance frequency occurs at about one-half

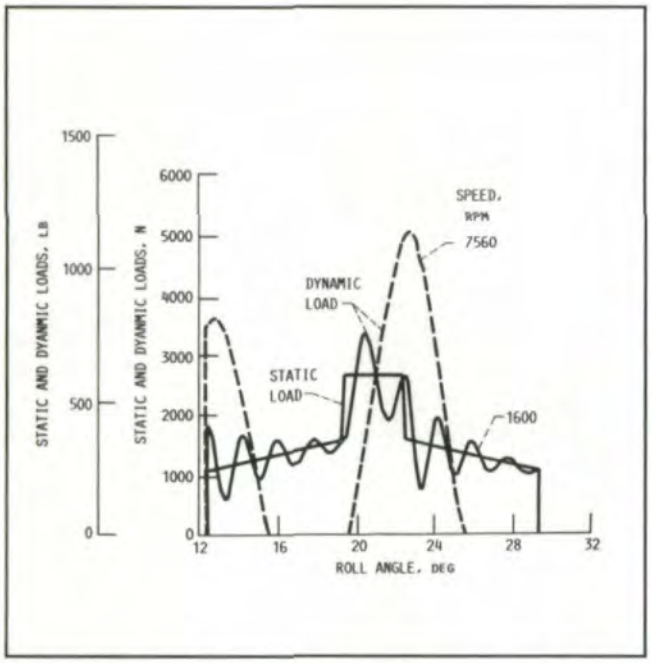

Fig. 3 – Dynamic loads at different speeds for identical years. Module = 3.18 mm; pressure angle = 20°; pitch radii = 57.1 mm; applied load = 2760 N (600 lb.).

of the critical speed.[2] For speeds above the critical speed, the dynamic response decreases steadily in the same manner as with elementary vibrating systems.

Fig. 5 shows a three-dimensional representation of the system dynamic response. The horizontal axis represents the operating speed, and the contact position along the tooth profile. The total number of contact positions is 121. The vertical axis is the dynamic factor.

Fig. 6 presents a contour plot of the system dynamic response. The shaded areas represent regions where tooth separation occurs. They are located in the double contact regions. At near resonance speeds the vibration amplitude exceeds the deflection of the meshing teeth, thus inducing tooth separation.

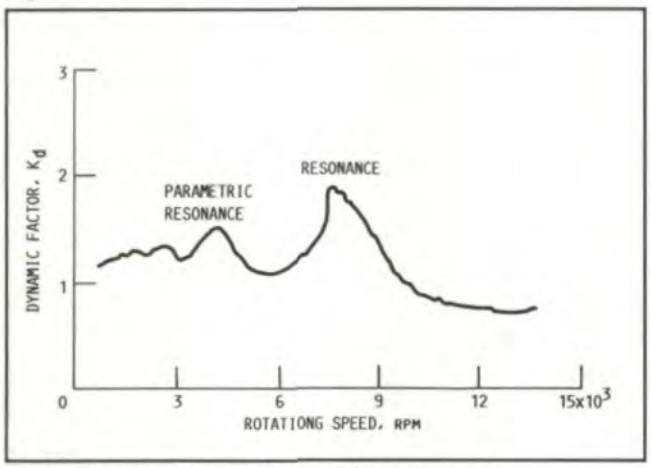

Fig. 4 – Dynamic factor as a function of rotating speed.

As the speed increases, the dynamic response also shows a phase shift toward the higher numbered contact positions. This phenomenon can be seen by noting that at speeds from 600 to 4200 rpm (one-half subharmonic), the maximum dynamic load occurs at double- to single-contact transitions (position 51) and gradually changes to single- to double-contact transitions (position 75). At speeds between one-half subharmonic and resonance, the maximum peak stays near the single- to double-contact transitions. After the speed

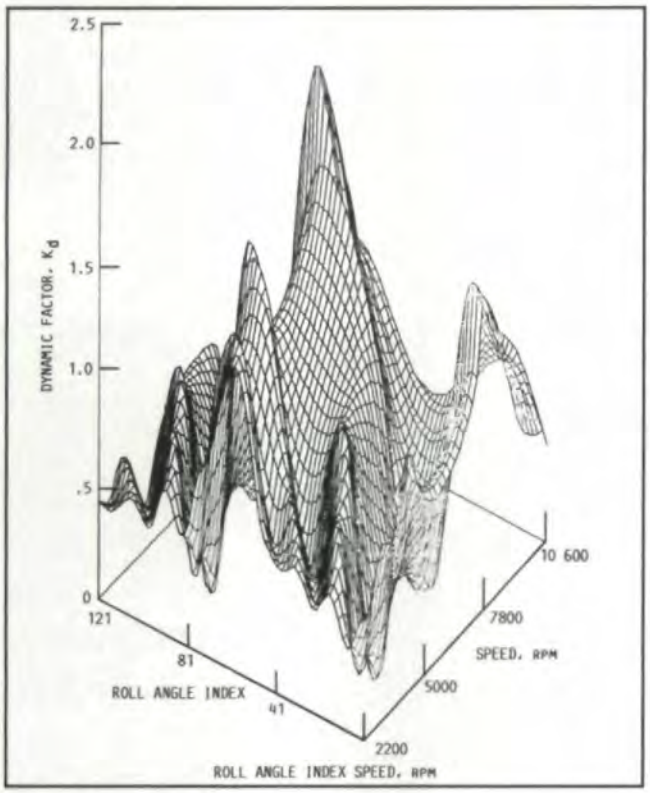

Fig. 5 – System dynamic response.

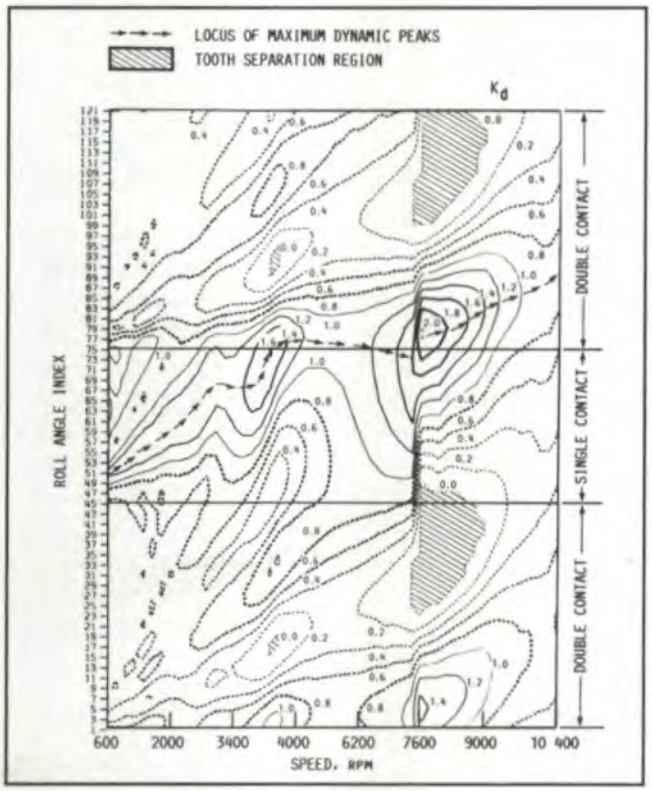

Fig. 6 – Contour plot of system dynamic response.

passes resonance, the major dynamic peak moves again towards higher contact positions on tooth profile with increasing speed.

Fig. 7 shows the dynamic factor as a function of the transmitted loads for three different speeds. There is only a small decrease in dynamic factor with increased applied load.

Fig. 8 shows the effect of damping on the dynamic load. It is seen that damping has its greatest effect near resonance frequencies.

Changes in shaft stiffness have a minor effect on the system dynamic response. However changes of tooth stiffness have a major effect on the response. Fig. 9 shows that the higher the tooth stiffness the lower the dynamic response (dynamic factor). This is consistent with observations that as the tooth

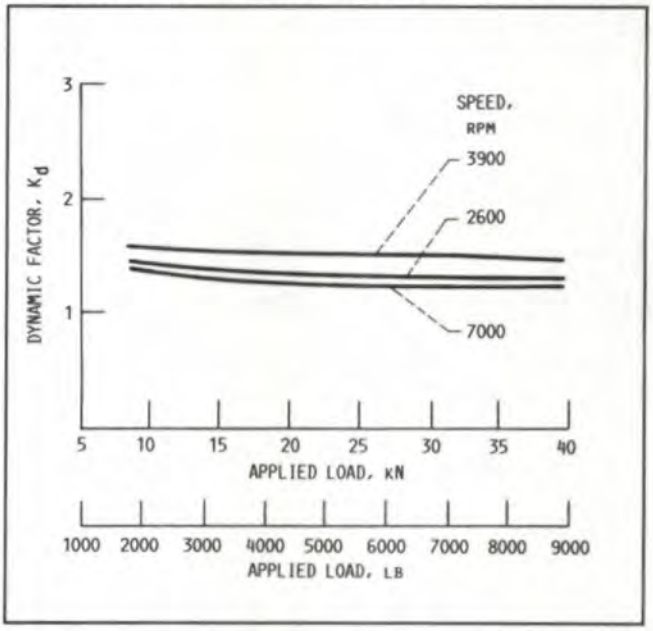

Fig. 7 – Effect of applied load on dymanic response.

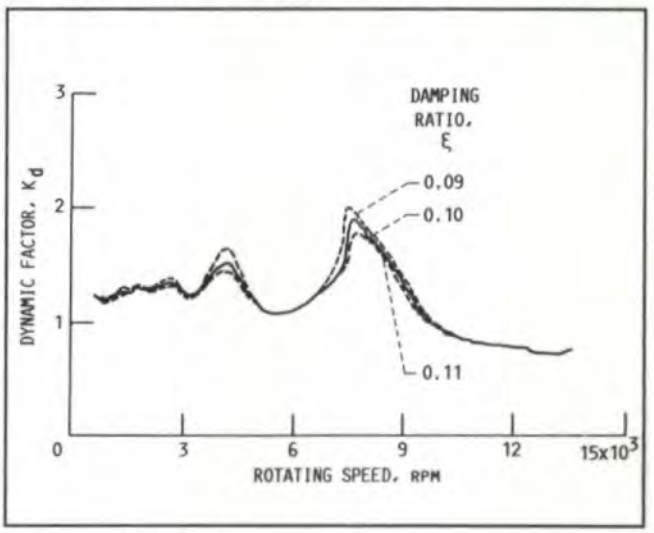

Fig. 8 – Effect of damping on dynamic response.

stiffness increases the effect of gear mass on the system dynamics is reduced. Fig. 9 also shows that system resonance frequencies are increased as the tooth stiffness increases. This is a potentially useful effect for the design of gear systems.

The effect of shaft mass is assumed small compared to that of the gears. Fig. 10 shows that as the gear inertia is reduced, the dynamic response is also reduced.

For gears with different diametral pitches, the dynamic response is different due to the change in contact ratio. Gears with a finer pitch have a higher contact ratio. Since the contact ratio is a measure of the duration of the load being shared by more than one pair of teeth, it has a significant effect on the system dynamic response.

Fig. 11 shows a comparison between gears having different diametral pitches. The finer pitch gears, having a higher contact ratio, have a smaller dynamic load than the coarser pitch gears.

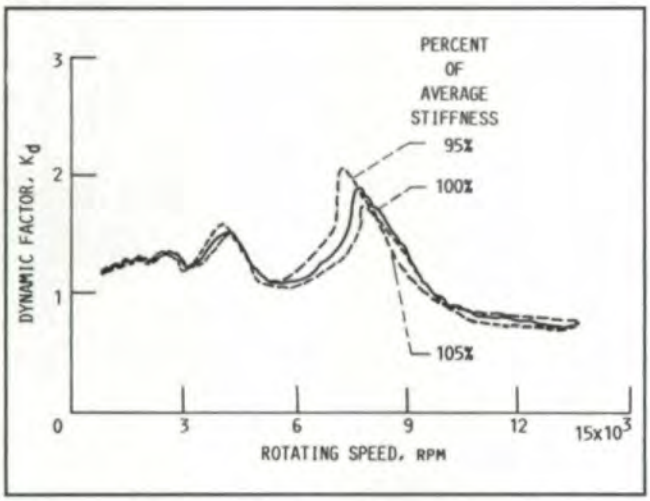

Fig. 9 – Effect of average tooth stiffness on dynamic response. Average tooth stiffness: 100% value = 3.991×10^5 N-m/rad.

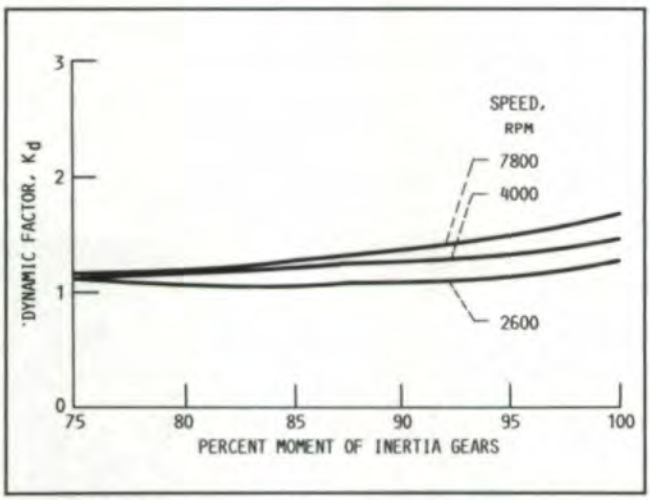

Fig. 10 – Effect of gear inertia on dynamic response. (Gear inertia: 100% value = 3.33×10^{-3} kg – m^2).

CIMA USA YOUR SOURCE FOR WORLD CLASS GEARMAKING TECHNOLOGY...

... lets you select familiar component systems

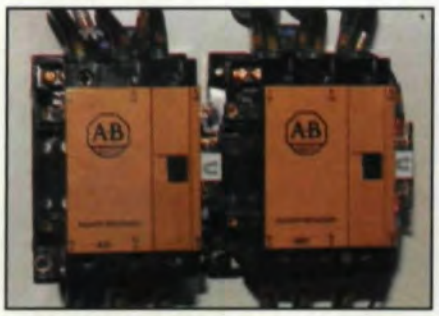

When you order a CIMA 6-axis gear hobber… you get to make lots of choices (if you want to). We'll let you choose from a wide variety of controls, hydraulics, electrical components and other critical systems so set-up, routine maintenance and machine adjustments can be made quickly and easily with your own staff.

Our World Class gearmaking systems combine the best of state-of-the-art component technology and user friendly operation with rugged, reliable machine designs… for years of optimum performance. Our newest model, the…

CIMA CE 260 CNC6 hobs gears up to 10-1/2" OD from a compact, new, 71 sq. ft. footprint. Certainly no "light-weight", the new generation 260 Series Hobber offers a patented, new, table drive mechanism with a larger part-to-drive ratio, a fully engaged hob head slide and a wider hob head mechanism. All provide for greater workpiece stability… and optimized tooth-to-tooth spacing accuracy. CIMA also includes standard features like: 6 axis operation, full thermal compensation, air-conditioned cabinetry, 4 synchronized software control options, and semi-automatic hob changing. With options for tangential feeding, fully automatic hob changing, automatic fixture change and a host of loading configurations, CIMA-USA can custom-build a machine to match your exact specifications. After all…

Great American gearmakers deserve world class machines that are built… to REDUCE CYCLE TIMES, IMPROVE & MONITOR QUALITY and INCREASE SHOP PROFITABILITY. Given the choice… isn't that what you want for your gear shop??

Compact Footprint

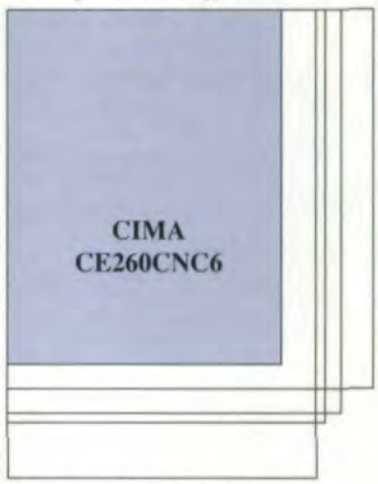

Comparable 250–300mm machines consume up to 80% more floor space.

Ask our representative for a copy of our latest brochure, or contact:

CIMA-USA
Division of GDPM Inc.
501 Southlake Blvd.
Richmond, VA 23236
Phone (804) 794-9764
FAX (804) 794-6187
Telex 6844252.

CIMA USA

Global Technology with a U.S. Base

CIRCLE A-14 ON READER REPLY CARD

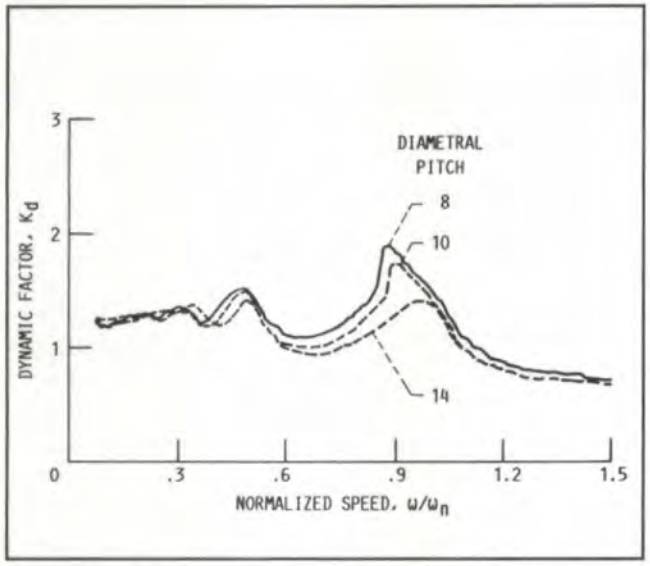

Fig. 11 – Effect of diametral pitch on dynamic response.

Discussion

In 1927, A.A. Ross[3] introduced the following empirical formula for the dynamic factor k_v:

$$k_v = \frac{78}{(78 + \sqrt{v})} \tag{9}$$

where v is the pitch line speed measured in ft/min. This expression received acceptance as a standard factor used by the American Gear Manufacturer's Association (AGMA). In 1959, a similar factor for use with higher precision gears was introduced by Wellauer.[4]

$$k_v = \left[\frac{78}{78 + \sqrt{v}}\right]^{1/2} \tag{10}$$

Equations 9 and 10 are recognized as being conservative when applied with very high precision gears. They are thought to predict dynamic loads which are higher than the actual loads.

Buckingham[5] has also developed an expression for the dynamic load in terms of the pitch line speed and the applied load. His formula is

$$W_d = W + [f_a(2f_b - f_a)]^{1/2} \tag{11}$$

where W_d is the dynamic load, W is the applied load, and the factors f_a and f_b are

$$f_a = f_b f_c/(f_b + f_c) \text{ and } f_b = 0.0000555\,EF + W \tag{12}$$

where F is the face width, E is the elastic constant, and f_c is

$$f_c = 0.00120\,[(R_1 + R_2)/R_1R_2]mv^2 \tag{13}$$

where R_1 and R_2 are the pitch radii of the gears, and m is their effective mass. (In these expressions the units are in pounds and inches except for the pitch line speed which is measured in ft/min.)

Kubo[6] measured static and dynamic gear stresses on several high-precision spur gear systems. Kubo expressed the dynamic factor as the ratio of maximum dynamic to the maximum static stress. Since stress is proportional to load, Kubo's definition of dynamic factor is identical to that used here. Fig. 12 shows a comparison of $(1/K_v)$ from the AGMA high-precision formula (Equation 10), (W_d/W) from Buckingham's formula, Kubo's results, and the results of the computer simulation for an identical spur gear pair with 4 mm module, 25 teeth, 20° pressure angle, 15 mm face width, 131.5 kN/m applied load, and 207 GPa Young's modulus.

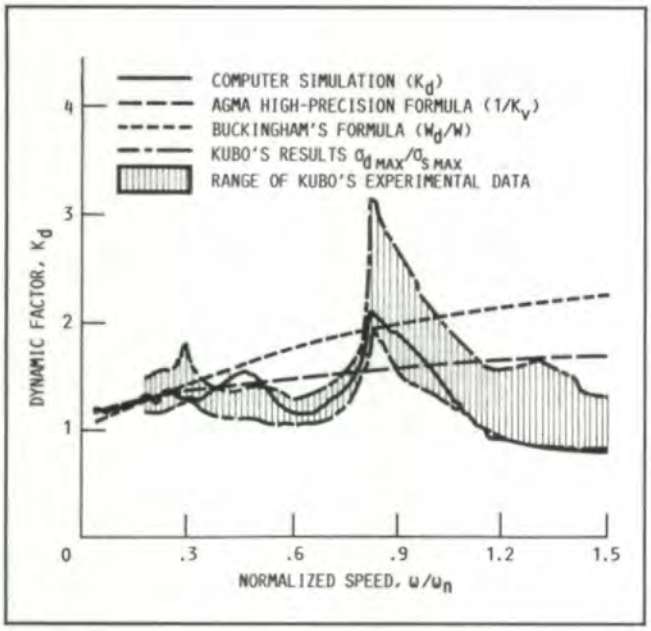

Fig. 12 – Comparison of experimental, empirical, and computer simulation results.

There is a good agreement between Kubo's result and the computer simulation.

Conclusions

From the foregoing results several conclusions may be stated:

1. For accurately made gears, the dynamic load is significantly affected by the contact ratio: for increased diametral pitch, that is, for high contact ratio gears, the dynamic load is decreased.

2. The tooth stiffness has a significant effect upon the dynamic load: the higher the stiffness, the lower the dynamic load. Also, the higher the stiffness, the higher the critical speed for peak response.

3. The dynamic load generally increases with the operating speed until a resonance is reached. The dynamic load decreases rapidly beyond the resonance.

4. Damping and friction decrease the dynamic load with the most dramatic effects occurring near the resonance frequencies.

5. The applied load has a relatively minor effect upon the dynamic factor.

6. Tooth separation – leading to impact – occurs in the double tooth contact region since the deflections are smallest in that region.

7. The dynamic factor is largest for contact points near the tooth tip.

8. The dynamic factor decreases with decreases in the gear body inertia. Shaft moment of inertia has a minimal effect upon the dynamic factor.

References:

1. LIN, H.H., HUSTON, R.L., and COY J.J. "On Dynamic Loads in Parallel Shaft Transmissions. I - Modeling and Analysis." NASA TM-100180, 1987. Also *Gear Technology*, Vol. 7, No. 1, Jan/Feb, 1990.
2. NAFEH, A.H. and MOOK, D.T. *Nonlinear Oscillations*. Wiley, 1979, Chapt. 5.
3. ROSS, A.A. "Tooth Pressures for High-Speed Gears." *Machinery* (NY), Vol. 34, No. 2, Oct. 1927, pp. 110-112.
4. WELLAUER, E.J. "An Analysis of Factors Used for Strength Rating of Helical Gears." *J. Eng. Ind.*, Vol. 82. No. 3, Aug. 1960, pp. 205-212.
5. BUCKINGHAM, E. *Analytical Mechanics of Gears*. Dover, 1963.
6. KUBO, A. "Estimation of Gear Performance." *Proceedings of the International Symposium on Gearing and Power Transmissions*. Japan Society of Mechanical Engineers, Tokyo, 1981, pp. 201-206.

Acknowledgements: Published in *ASME Journal of Mechanisms, Transmissions, and Automation in Design*, Vol 110, No. 2, June, 1988, pp. 221-229, and as NASA Technical Memorandum 100281 and AVSCOM T.M. 87-C-3. Reprinted with permission.